Fold-Unfold Transitions in the Selectivity and Mechanism of Action of the N-Terminal Fragment of the Bactericidal/Permeability-Increasing Protein ($rBPI_{21}$)

Marco M. Domingues,[†] Sílvia C. D. N. Lopes,[‡] Nuno C. Santos,[†] Alexandre Quintas,[§] and Miguel A. R. B. Castanho[†*]

[†]Instituto de Medicina Molecular, Faculdade de Medicina da Universidade de Lisboa, Lisbon, Portugal; [‡]Centro de Química-Física Molecular, Instituto Superior Técnico, Lisbon, Portugal; and [§]Instituto Superior de Ciências da Saúde Egas Moniz, Monte da Caparica, Portugal

ABSTRACT Septic or endotoxic shock is a common cause of death in hospital intensive care units. In the last decade numerous antimicrobial peptides and proteins have been tested in the search for an efficient drug to treat this lethal disease. Now in phase III clinical trials, $rBPI_{21}$, a recombinant N-terminal fragment of the bactericidal/permeability-increasing protein (BPI), is a promising drug to reduce lesions caused by meningococcal sepsis. We correlated structural and stability data with functional information of $rBPI_{21}$ bound to both model systems of eukaryotic and bacterial membranes. On interaction with membranes, $rBPI_{21}$ loses its conformational stability, as studied by circular dichroism. This interaction of $rBPI_{21}$ at membrane level was higher in the presence of negatively charged phospholipid relatively to neutral ones, with higher partition coefficients (K_p), suggesting a preference for bacterial membranes over mammalian membranes. $rBPI_{21}$ binding to membranes is reinforced when its disulfide bond is broken due to conformational changes of the protein. This interaction is followed by liposome aggregation due to unfolding, which ensures protein aggregation, and interfacial localization of $rBPI_{21}$ in membranes, as studied by extensive quenching by acrylamide and 5-deoxylstearic acid and not by 16-deoxylstearic acid. An uncommon model of the selectivity and mechanism of action is proposed, where membrane induces unfolding of the antimicrobial protein, $rBPI_{21}$. The unfolding ensures protein aggregation, established by protein-protein interaction at membrane surface or between adjacent membranes covered by the unfolded protein. This protein aggregation step may lead to membrane perturbation.

INTRODUCTION

Gram-negative bacteria have two cell envelope membranes. The outer membrane is asymmetric, with the glycolipid lipopolysaccharide (LPS) covering >90% of its outer leaflet surface and the inner leaflet with a phospholipid composition similar to the cytoplasmic membrane (1,2). The highly packed LPS moieties confer bacteria resistance to most antimicrobial peptides. Nevertheless, many antimicrobial cationic peptides have been shown to interact with LPS of Gram-negative bacteria and sometimes pass across this membrane by self-promoted uptake, followed by interaction and insertion into the negatively charged cytoplasmic membrane (3,4). When present in the mammalian bloodstream, LPS elicits a common but often fatal condition named septic or endotoxic shock, characterized by hypotension and circulatory failure, which can culminate in multiple system organ failure. When in circulation, LPS, complexed with several different proteins (mainly lipopolysaccharide binding protein [LBP]), is recognized by CD14 receptors in macrophages, monocytes or neutrophils, which triggers a cascade of events that leads to sepsis (5–7). Sepsis is a combination of both local and systemic inflammatory responses, which requires a multipronged interventional strategy to contain the various phases of disease progression. LPS sequestration by small peptides or proteins is an attractive interventional modality and many naturally occurring peptides (magainins, mellitins, cecropins, etc.) have intrinsic LPS binding activity (8–12). Most of these peptides may form amphipathic helices. Their cationic nature facilitates anchorage to the negatively charged bacterial surface, whereas their amphiphilicity and high helical propensity promote the formation of α-helices in membranes. Moreover, the insertion of such amphipathic α-helices in membranes underpins their membrane disruption activity. Two related proteins, bactericidal/permeability-increasing protein (BPI) and LBP are known to mediate the biological effects of LPS and participate in the innate immune response to bacterial infection in different ways (13–15). LBP promotes LPS transfer to innate immune cells, activating them, whereas BPI, present in azurophil granules of polymorphonuclear neutrophils, acts as a cytotoxic agent against Gram-negative bacteria and neutralizing the toxicity of LPS (16,17). The N-terminal fragment of BPI ($rBPI_{21}$) not only maintains the biological activity, neutralizing LPS (18–21), but also represents a promising clinical tool to act against meningitis and septic shock (22). $rBPI_{21}$ is a recombinant 21 kDa truncated protein corresponding to amino acids residues 1–193 of the N-terminal of human BPI (with the exception that a cysteine is replaced by an alanine at position 132). Although various studies with BPI and its fragments have been carried out, namely concerning antimicrobial activity, there is still a great lack of information concerning its mode of action, specially at membrane level. The interaction of $rBPI_{21}$ with negatively charged lipids was reported

Submitted May 12, 2008, and accepted for publication October 17, 2008.

*Correspondence: macastanho@fm.ul.pt

Editor: Alberto Diaspro.

0006-3495/09/02/0987/10 $2.00

doi: 10.1016/j.bpj.2008.10.044

(23,24) but detailed structural information on the interaction with LPS is needed for the development of more effective endotoxin-neutralizing agents.

In this study, fluorescence spectroscopy, circular dichroism (CD) and light scattering were combined to systematically study the interaction of $rBPI_{21}$ with model systems of both eukaryotic and bacterial membranes, mainly: 1), the role of the disulfide bond and the selectivity to saccharide moiety of LPS regarding bounding/recognition of LPS by $rBPI_{21}$; 2), temperature effects on the binding to negatively charged groups of phospholipid bilayers; 3), the interaction with membranes of different compositions, as a key to understand the selectivity toward bacteria and; 4), the $rBPI_{21}$ conformational changes in its interaction with phospholipid membranes and/or LPS.

MATERIALS AND METHODS

$rBPI_{21}$, 99% pure, was a gift from XOMA Ltd. (Berkeley, CA). All lipids were obtained from Avanti Polar Lipids (Alabaster, AL), except LPS (*Escherichia coli* O55:B5) that was purchased from Fluka (Buchs, Switzerland). Dodecyl 2,6-dideoxy-β-L-*arabino*-hexopyranoside (DAHP) was a kind gift from Prof. Pilar Rauter (University of Lisbon, Portugal) and synthesized as described elsewhere (25). Acetate buffer (5 mM sodium acetate, 150 mM NaCl) was used in all the fluorescence studies. Sodium phosphate buffer was used instead of acetate buffer in the CD studies to prevent significant absorption interferences. Tris(2-cyanoethyl)phosphine (TCP) was from Molecular Probes (Eugene, OR). 5-deoxylstearic acid (5NS), 16-deoxylstearic acid (16NS), guanidinium chloride (GdnHCl), sodium phosphate, and all other chemicals were of the highest commercially available purity and were purchased from Sigma (St. Louis, MO). UV-Vis absorption measurements were carried out in a Shimadzu spectrophotometer (model UV-3101 PC), unless otherwise stated. Fluorescence spectroscopy measurements were conducted on a spectrofluorimeter SLM-Aminco 8100, equipped with a 450 W Xe Lamp and double monochromators in both excitation and emission, as well as a quantum counter.

Large unilamellar vesicles preparation

Large unilamellar vesicles (LUV), with ~100 nm of diameter, were obtained by extrusion of multilamellar vesicles as described elsewhere (26).

Fluorescence decays

Time-resolved fluorescence decay measurements were carried out as described previously (27) with a time-correlated single-photon counting system using a Hamamatsu R-2809 MCP photomultiplier (Hamamatsu, Japan) for the detection. Excitation and emission wavelengths of 285 nm and 308 nm, respectively, were chosen for $rBPI_{21}$ studies. $rBPI_{21}$, stock solution of 95.2 μM, was added to previously prepared vesicle suspensions to a final concentration of 0.7 μM. Fluorescence decays were complex and described by a sum of three exponentials. The mean lifetime, $\overline{\tau}$, was obtained from Eq. 1 (28):

$$\overline{\tau} = \frac{\sum a_i \tau_i^2}{\sum a_i \tau_i}, \tag{1}$$

where a_i and τ_i are the pre-exponential factors and the fluorescence life-time components, respectively.

The extent of incorporation of $rBPI_{21}$ in model system of eukaryotic and bacterial membranes

Partition studies were carried out in LUV, prepared using different lipids (phospholipid + glycolipid or phospholipid + lipopolysaccharide). $rBPI_{21}$ concentration was kept constant (0.7 μM). Fluorescence intensity was measured with excitation and emission wavelengths of 295 nm and 338 nm, respectively. The measured fluorescence intensity, I_f, is a balance between the fluorescence intensities of the peptide in aqueous phase (I_W) and inserted in the lipid matrix (I_L) as follows Eq. 2 (29). The weight factors in this balance depend on the partition coefficient, K_p, which was calculated as a fit parameter in a nonlinear regression methodology.

$$\frac{I_f}{I_W} = \frac{1 + K_p \gamma_L [L](I_L/I_W)}{1 + K_p \gamma_L [L]} \tag{2}$$

$$K_p = \frac{\frac{n_{S,L}}{V_L}}{\frac{n_{S,W}}{V_W}} = \frac{[Peptide]_L}{[Peptide]_W}, \tag{3}$$

where $[L]$ the lipid molar concentration and γ_L denotes the molar volume of the lipid; $n_{S,i}$ are the moles of the solute present in each phase ($i = L$ and $i = W$ refer to the lipid and aqueous media, respectively).

In this work we studied the lipid phase influence on $rBPI_{21}$ partition to different model systems of membranes. We wanted to study not only the influence of the lipid phase (liquid-crystalline versus gel) but also the electrostatic effect (negative charged lipids versus zwitterionic lipids) and the influence of different kinds of negatively charged lipid headgroups (phosphatidylglycerol versus phosphatidylserine). Moreover we wanted to compare LPS with an unrelated membrane bound saccharide (dihydroxyacetone phosphate [DHAP] versus LPS). palmitoyloleoylphosphatidylcholine (POPC) and palmitoyloleoylphosphatidylglycerol (POPG) LUV are in liquid-crystalline phase whereas dipalmitoylphosphatidylcholine (DPPC), dipalmitoylphosphatidylglycerol (DPPG), and dipalmitoylphosphatidylserine (DPPS) LUV are in gel phase at 25°C and 37°C.

Fluorescence quenching studies of $rBPI_{21}$ in aqueous phase and model system of bacterial membranes

Acrylamide 8 M was used to quench $rBPI_{21}$ fluorescence in the aqueous phase. $rBPI_{21}$ was dissolved in acetate buffer, pH 6.5 or 7.4. Aliquots of acrylamide were added to the mixture up to 0.5 M and the fluorescence intensity was measured at 325 nm. Quenching experiments with acrylamide were carried out to study Trp residues exposure to the aqueous phase. Acrylamide was added to samples containing $rBPI_{21}$ and LUV of phospholipids with or without DAHP or LPS up to 0.5 M. Data treatment was as described elsewhere (30). Fluorescence intensity was measured with excitation and emission wavelengths of 295 nm and 330 nm, respectively. Differential quenching studies were carried out to study the in-depth location of $rBPI_{21}$ in LUV of phospholipids with or without DHAP or LPS (both were in final 5%, molar, of the total lipid concentration). These quenching studies were carried out by adding small aliquots of 5NS or 16NS (70 mM solutions in ethanol) to the suspension of LUV with $rBPI_{21}$ added previously. Ethanol was kept below 2% (v/v) to not affect lipid vesicles structure. When inserted in lipid bilayers, 5NS and 16NS have doxyl moieties close to the headgroup region and in the acyl chain region of the lipid palisade, respectively.

The simplest model that describes dynamic or static fluorescence quenching leads to linear Stern-Volmer plots:

$$\frac{I_0}{I} = 1 + K_{SV}[Q], \tag{4}$$

where I_0 and I denote the fluorescence intensities without and with quencher, respectively, K_{SV} is the Stern-Volmer constant and $[Q]$ is the quencher concentration. However, nonlinear Stern-Volmer plots are observed when there are multiple classes of fluorophores (31), such as a fluorophore population protected from the contact of the quencher and a population that is accessible to it (32).

The role of the disulfide bond of $rBPI_{21}$ both in its structure in solution and in the extent of incorporation in model systems of bacterial membranes

TCP solution was prepared by dilution in acetate buffer. For modification with TCP in solution, $rBPI_{21}$ was dissolved in acetate buffer, pH 6.5 or 7.4. Aliquots of TCP were added to the mixture at fixed intervals and fluorescence spectra were recorded. The final concentration of TCP ranged from 0.2 to 1.4 mM. To study the influence of a reduction in $rBPI_{21}$ extent of incorporation in model systems of bacterial membranes, $rBPI_{21}$ was preincubated with TCP (final concentration 1.4 mM) and added to LUV composed of POPC/POPG/DAHP or POPC/POPG/LPS. Fluorescence intensity was measured afterward and partition coefficients were calculated.

Conformational studies of $rBPI_{21}$ in aqueous phase and in model systems of bacterial membranes by CD

Secondary structure analysis was carried out by far-UV (185–260 nm) CD in a Jasco J810 Spectropolarimeter (Jasco, Japan) equipped with a temperature control unit Julabo F25. Far UV CD spectra were recorded with 0.1 cm (linear) path length quartz cuvette. For each spectrum, three scans were averaged. $rBPI_{21}$ samples in 20 mM sodium phosphate buffer with 150 mM sodium fluoride, pH 6.5 or 7.4, in the presence or absence of 0.1 mM lipid concentration were equilibrated either at 25°C or 37°C, before measurements. Minor contributions of circular differential scattering were eliminated by subtracting the CD spectrum of buffer and/or lipids from the peptide spectrum on buffer and lipids, respectively. For $rBPI_{21}$ secondary structure estimation, CD spectra were deconvoluted using the CDSSTR algorithm (33) on Dichroweb (34).

Conformational stability measurements

$rBPI_{21}$ conformational stability studies were carried out by CD in GdnHCl-induced protein unfolding experiments either at 25°C or 37°C, at pH 6.5 and pH 7.4, after 48 h of incubation. CD denaturation curves were constructed using the ellipticity at 222 nm. A nonlinear least squares fitting procedure yielded values for $\Delta G^0(H_2O)$, the conformational stability, and m, the dependence of ΔG^0 on denaturant concentration. C_m, the denaturant concentration at the midpoint of the unfolding transition was calculated as $C_m = \Delta G^0(H_2O)/m$ and K_U, the unfolding equilibrium constant, was calculated as $K_U = e^{-\Delta G^0(H_2O)/RT}$ (35). Denaturation curves for monomeric species were analyzed considering the equation developed by Santoro and Bolen (36). Parameters were obtained by fitting the derived equations to experimental data by nonlinear regression using the solver add-on for Microsoft Excel 2003 (Microsoft, Redmond, WA).

Aggregation of negatively charged vesicles in the presence of $rBPI_{21}$ by dynamic light scattering

Dynamic light scattering experiments were carried out on a Malvern Zetasizer Nano ZS (Malvern Instruments, Worcestershire, UK) with a backscattering detection at 173° and equipped with He-Ne laser ($\lambda = 632.8$ nm), at 37°C, using disposable polystyrene cells. The phosphate buffer and lipid were mixed and then filtered in a syringe filter with pore size of 0.45 μm (Whatman, Florham Park, NJ). Lipid concentration was fixed at 50 μM and the $rBPI_{21}$ concentration was varied from 24 nM to 238 nM. The samples were left equilibrating for 30 min at 37°C. Normalized intensity autocorrelation functions were analyzed using the CONTIN method (37,38) yielding a distribution of diffusion coefficients (D) in the whole solution through multiexponential fits. The measured D is used for the calculation of the hydrodynamic radius (R_H) through the Stokes-Einstein relationship:

$$D = \kappa T/6\pi\eta R_H, \quad (5)$$

where κ is the Boltzmann constant, T the absolute temperature, and η the medium viscosity. The hydrodynamic diameter (D_H) of the sample was obtained from the peak with the highest scattered light intensity in light scattering intensity distributions.

RESULTS AND DISCUSSION

Studies in aqueous solution

On excitation at $\lambda \geq 295$ nm, the fluorescence of $rBPI_{21}$ is dominated by tryptophan fluorescence, either at pH 6.5 or 7.4. In buffer solution the Trp emission of $rBPI_{21}$ occurs at shorter wavelengths, relative to the emission of Trp in aqueous environment (Table 1). This blue shift results from the shielding of the Trp residues from water by the hydrophobic core of the folded peptide. BPI structure shows a Trp residue in hydrophobic environment (39), which may explain both this large blue shift and the increased fluorescence lifetime (Fig. 1). In buffer solution, intrinsic fluorescence emission was decreased for pH 6.5, although no shift in the fluorescence spectra is observed. This result suggests that a slightly acid pH induces conformational changes that induce self-quenching but do not involve exposure of the Trp residues to the aqueous medium.

TCP was added to $rBPI_{21}$ solution to study eventual changes in the Trp environment after the breaking of the disulfide bond. At pH 6.5 the emission maximum occurs at a higher wavelength (Fig. 2 *A*), on addition of TCP. This red shift suggests a change in the Trp residue environment to a more hydrophilic one. This is a combined effect of lowering the pH, which is close to histidines pK_a, and disulfide bond breaking. No significant difference was observed in the emission spectra at pH 7.4 (Fig. 2 *B*), on addition of TCP, which points out to the fact that although disulfide bond reduction may induce conformational changes, these do not globally affect the Trp environment at this pH. These results in aqueous solution show that $rBPI_{21}$ undergoes conformational changes when both acidification and disulfide bond reduction occurs, where $rBPI_{21}$ exposes the Trp to a more hydrophilic environment.

$rBPI_{21}$ conformation and stability in aqueous buffer solution

To know if $rBPI_{21}$ is folded at 37°C, thermal stability runs followed by CD were carried out (results not shown). The

TABLE 1 Photophysical parameters for Trp and $rBPI_{21}$, in acetate buffer and in large unilamellar vesicles (5 mM), at pH 7.4

Parameters	Trp	$rBPI_{21}$
λ_{Abs}/nm	280*	276
λ_{Em}/nm	348*	325
$\overline{\tau}_W$/ns	2.6*	5.7
$\overline{\tau}_L$/ns	—	4.1

λ_{Abs}, λ_{Em} are maximum absorption and emission wavelengths, respectively, and $\overline{\tau}$ is the mean fluorescence lifetime. [Trp] = 1.0 mM; [$rBPI_{21}$] = 7.7 μM. W and L subscripts denote aqueous and lipid environments, respectively.
*At 23°C in aqueous solution at neutral pH (28).

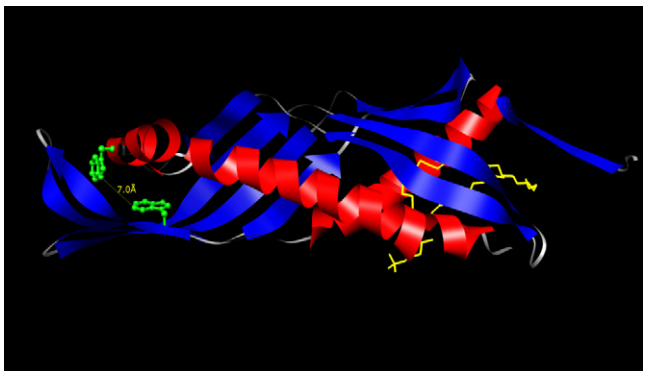

FIGURE 1 3D ribbon structure of the first 193 residues of BPI, corresponding to the sequence of the $rBPI_{21}$. Secondary structure of the α-helices is represented in red online and black in print, β-sheets are in blue online and dark gray in print. Phosphatidylcholine (*yellow* online and *gray* in print), is localized in the hydrophobic pocket of the protein, and tryptophan residues are represented in green online and as a ball and stick residue in print. Structure based on the crystallographic structure of BPI (44).

results show that $rBPI_{21}$ is in its native conformation in aqueous solution at 25°C and 37°C.

To address the importance of histidine protonation on the $rBPI_{21}$ structure, we have characterized the chemical conformational stability of $rBPI_{21}$ at pH 6.5 and 7.4. Fig. 3 shows the equilibrium denaturation curves at pH 7.4 and 6.5 at 25°C, using guanidinium chloride (GdnHCl) as denaturant, monitored by CD. The free energy of unfolding ($\Delta G^0(H_2O)$) was directly obtained by a nonlinear least-squares fit of the experimental fluorescence data to a two-state model for monomer unfolding (35,36). GdnHCl-induced denaturation of $rBPI_{21}$ was found to be reversible for both pH values studied, as judged by CD and fluorescence experiments. Analysis of GdnHCl-unfolded $rBPI_{21}$ samples after dialysis, by CD and fluorescence, produced typical $rBPI_{21}$ spectra parameters. Table 2 shows the values obtained from the curves in Fig. 3 for $\Delta G^0(H_2O)$, the conformational stability, m, the dependence of ΔG^0 on denaturant concentration, and C_m, the denaturant concentration at the midpoint of the unfolding transition. The low values of $\Delta G^0(H_2O)$ for $rBPI_{21}$ are well within typical values of conformational stability for peptides and truncated proteins.

The lower $\Delta G^0(H_2O)$ values obtained at pH 6.5 indicates a decrease in the conformational stability of $rBPI_{21}$ when compared with the $\Delta G^0(H_2O)$ at pH 7.4 (Table 2). The smaller value of the conformational stability of $rBPI_{21}$ at pH 6.5 agrees completely with the higher tendency for denaturation of $rBPI_{21}$ at pH 6.5. Moreover, the denaturation midpoint, C_m, also shows this tendency, confirming the reduction of conformational stability on acidification.

It is worth noting that the slightly higher conformational stability shown by $rBPI_{21}$ at pH 7.4 is also due to a higher m (Table 2). The m value is believed to reflect the extent of newly exposed surface area on unfolding (40). Thus, the higher m value observed for the unfolding of $rBPI_{21}$ at pH 7.4 may indicate a more compact structure when compared

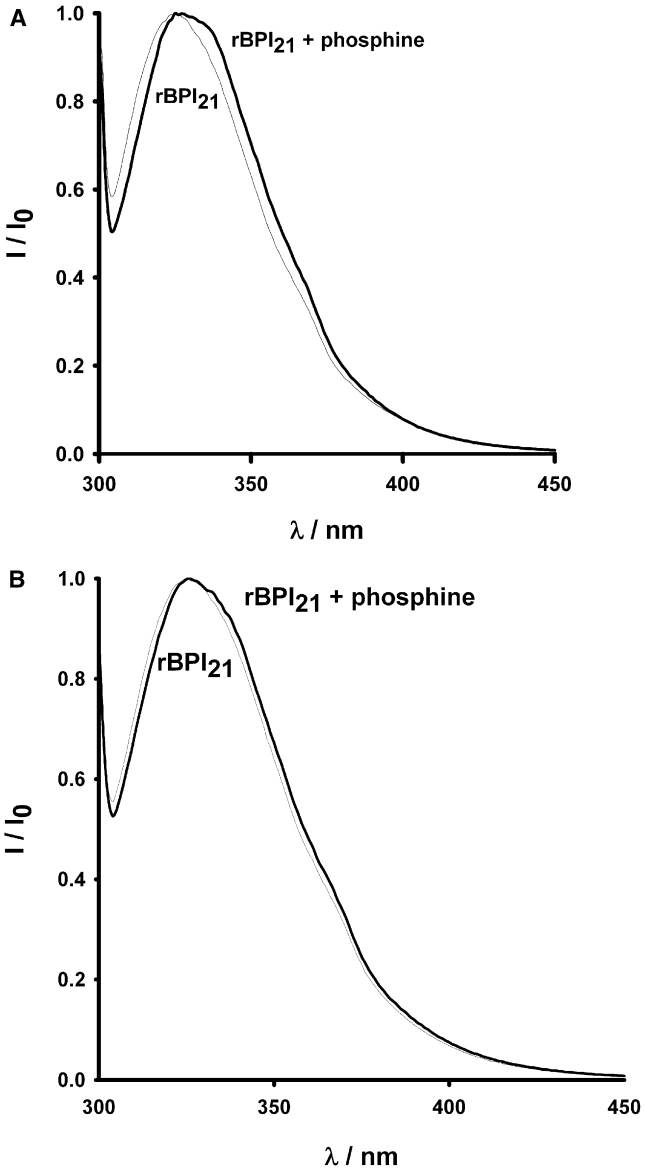

FIGURE 2 $rBPI_{21}$ (7.7 μM) fluorescence emission spectra in acetate buffer before and after incubation with TCP (1.4 mM). (*A*) pH 6.5. (*B*) pH 7.4. λ_{exc}= 295 nm, at 37°C. Similar spectra were obtained at 25°C.

with $rBPI_{21}$ conformation at pH 6.5, which is in agreement with the results obtained from fluorescence techniques.

Interaction of $rBPI_{21}$ with model systems of eukaryotic and bacterial membranes

Partition of $rBPI_{21}$ into model systems of eukaryotic and bacterial membranes was investigated from changes in the $rBPI_{21}$ intrinsic fluorescence, as described in Materials and Methods. Table 3 shows that $rBPI_{21}$ interacts more effectively with negatively charged membranes in the gel crystalline phase, the highest partition coefficients being obtained for DPPG, at 37°C, which may help to explain the preference of $rBPI_{21}$ for Gram-negative bacteria. These bacteria are known

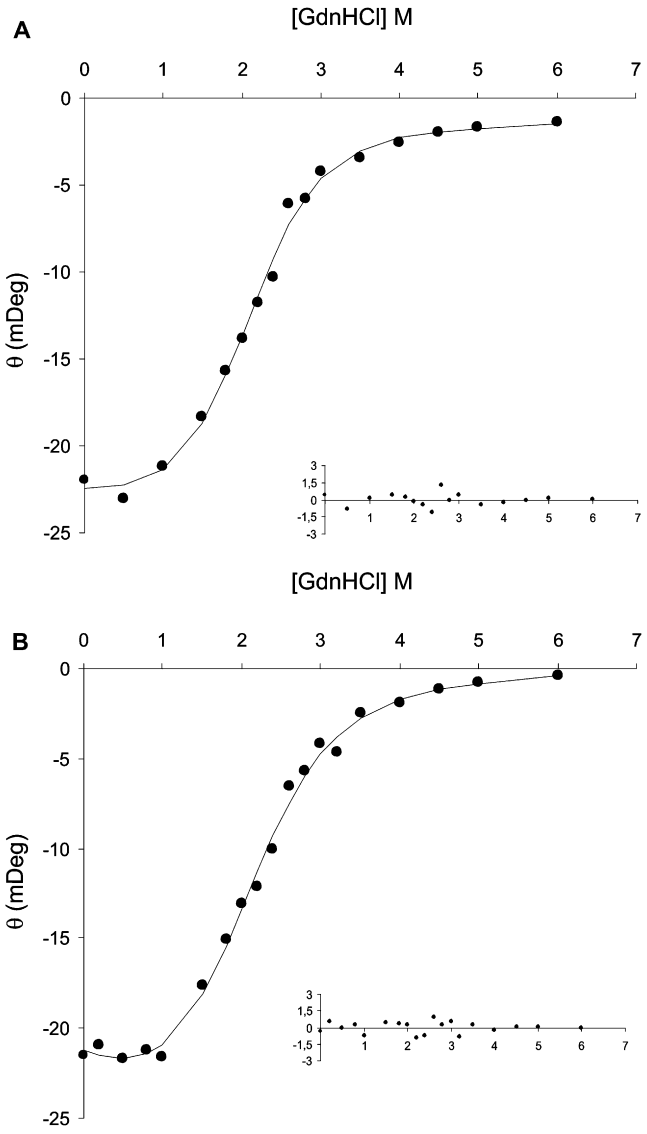

FIGURE 3 GdnHCl equilibrium denaturation curves of $rBPI_{21}$ at pH 7.4 (*A*) and 6.5 (*B*), at 25°C, monitored by CD at 222 nm. The curves are nonlinear least squares fits of an equation representing the entire denaturation curves, based on a two-state model and using the linear extrapolation method to the experimental CD data (36). Insets represent the residues of the fit to the experimental data.

for having an asymmetric outer membrane in which >90% of its outer leaflet surface is covered by LPS, which compared to typical phospholipid membranes are known to have tighter hydrocarbon chain packing and form rigid domains (41). The preference of $rBPI_{21}$ for gel phase membranes with high density of negative charges is remarkable and parallels $rBPI_{21}$ selectivity for the external surface of the outer membrane of gram-negative bacteria. The effect of charge alone does not suffice to explain this selectivity, as the partition coefficient for fluid POPG bilayers is considerably lower than the obtained for the rigid DPPG. Moreover, $rBPI_{21}$ is sensitive to the chemical nature of the headgroups. K_p differs in mixtures containing PG and PS, where $K_{p(PG)} > K_{p(PS)}$

TABLE 2 Stability parameters for $rBPI_{21}$ in aqueous solution, at pH 6.5 and 7.4, obtained from a direct fit of the experimental data in Fig. 3 to a two-state unfolding model

pH	$\Delta G^0(H_2O)$/kcal.mol^{-1}	C_m/M	m/kcal.mol^{-2} × L
6.5	2.05	1.90	1.07
7.4	2.68	2.04	1.31

$\Delta G^0(H_2O)$ is the free energy of unfolding, C_m, is the denaturant concentration at the midpoint of the unfolding transition, calculated as $C_m = \Delta G^0(H_2O)/m$, and m is the ΔG^0 dependence on the denaturant concentration.

(Fig. 4). This is of particular importance because PG is the major phospholipid component present in the cytoplasmic membrane of bacteria.

However, similar partition coefficients are obtained when LPS is replaced by an unrelated saccharide, which shows that $rBPI_{21}$ is rather insensitive to the glycidic group. POPC is the major lipid component of eukaryotic membrane cells. If we calculate the ratio $K_{p(\text{glycolipid or LPS systems})}/K_{p(POPC)}$ for $rBPI_{21}$ at physiological conditions (pH 7.4 and 37°C), values between 52 and 100 are obtained, which show clearly the preference of $rBPI_{21}$ for bacterial membranes. Curiously, for some lipid model systems higher partition coefficients were obtained at pH 6.5, relative to pH 7.4 (data not shown). Similar fluorescence emission and CD spectra were obtained for $rBPI_{21}$ at both pH values. However, a slight decrease in fluorescence intensity without a spectral shift was observed with pH decrease, which suggests that pH changes can induce an approximation between Trp and intramolecular quencher groups, rather than exposing Trp to the aqueous medium. Nevertheless, the exposure of hydrophobic segments is probably involved in the interaction of $rBPI_{21}$ with the target membrane. This hydrophobic segments exposure hypothesis provides what we believe is a new insight, if we remember that conformational stability studies (see section above) showed that there is a slight conformational stability reduction on acidification, and that at pH 6.5 $rBPI_{21}$ has a slightly less compact native state. Moreover, $rBPI_{21}$ has several His residues near a tryptophan residue. As pH 6.5 is near the pK_a value for His residues, protonation of His residues could generate positive charges on $rBPI_{21}$, which may contribute

TABLE 3 Partition coefficients (K_p) for $rBPI_{21}$ in different lipid systems at pH 7.4 and 37°C

System	$Kp \times 10^3$
DPPG	13.6 ± 5.00
DPPC/DPPG	9.75 ± 1.82
DPPC/DPPS	3.98 ± 1.18
DPPC	0.123 ± 0.054
POPG	0.851 ± 0.213
POPC	≈0
POPC/POPG/DAHP	0.52 ± 0.17
POPC/POPG/LPS	1.12 ± 0.073
POPC/POPG/DAHP (pre-incubated with TCP)	2.14 ± 0.71
POPC/POPG/LPS (pre-incubated with TCP)	4.64 ± 1.50

Anionic lipid contents in lipid mixtures: 50% molar; LPS or DAHP content in mixtures: 5%.

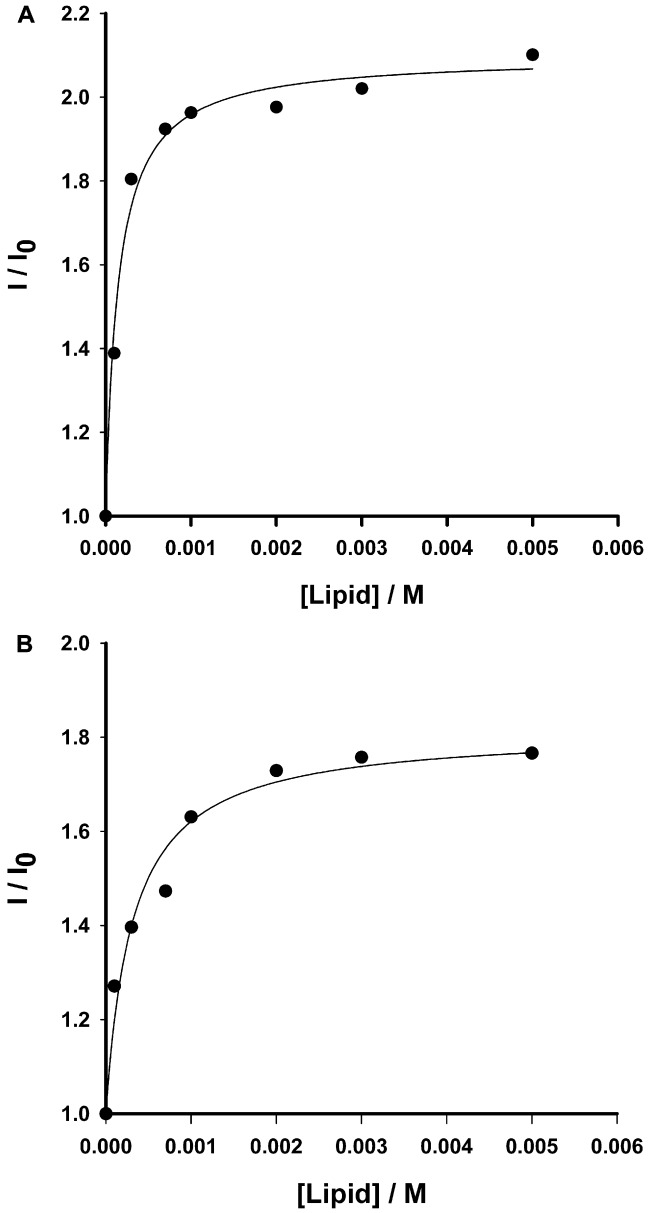

FIGURE 4 Determination of the partition constant (K_p) of the protein between the aqueous phase and phospholipid vesicles. Peptide concentration, of 0.7 μM, was constant during each set of experiments. Increase in fluorescence intensity obtained for different concentrations of (*A*) DPPC/DPPG and (*B*) DPPC/DPPS LUV. Fitting lines calculated using Eq. 2.

both to the reduction in the compactness of the protein, due to intercharge repulsion, and to the increase electrostatic interaction required for protein membrane binding. Consequently, K_p increases and potential quencher groups are formed.

Localization of rBPI$_{21}$ in model systems of bacterial membranes

The in-depth location of rBPI$_{21}$ in the model systems of bacterial membranes was studied by monitoring the relative quenching of the fluorescence of this peptide by the lipophilic spin probes 5NS and 16NS when inserted in fluid phase membranes of POPC/POPG/DAHP or POPC/POPG/LPS mixtures. The addition of any of the two nitroxide quenchers resulted in a decreased of rBPI$_{21}$ fluorescence intensity. The Stern-Volmer plots of the fluorescence intensity changes were linear (Fig. 5), indicating that nearly all rBPI$_{21}$ is inserted in the membrane at the used lipid concentration. The Stern-Volmer constants were obtained from their slopes. The ratio of these slopes, $K_{SV(5NS)}/K_{SV(16NS)}$ was found to be always higher than 1, pointing toward a shallow location of the peptide, except for the POPC/POPG system at pH 7.4 (Table 4).

In the case of the two bacterial model membranes composed of POPC/POPG/DAHP (or LPS) at physiological conditions (pH 7.4 and 37°C) the ratios obtained are quite similar (2.25 and 2.74 for the glycolipid and the LPS containing systems, respectively). This is indicative that rBPI$_{21}$ location is not LPS-specific.

To confirm the membrane location of rBPI$_{21}$, we used the hydrophilic quencher acrylamide, which quenches molecules present in the aqueous phase or in the lipid/water interface. rBPI$_{21}$ is more extensively quenched by acrylamide in lipid vesicles than in buffer solution, for all the lipid systems tested (data not shown). This result is in agreement with a shallow location of rBPI$_{21}$ in lipid vesicles, with an extended conformation where the Trp residues are relatively unshielded and more exposed to the aqueous environment than in the unbounded folded conformation. Tobias et al. (42) showed that BPI can increase the apparent size of LPS aggregates at 1:20 BPI/LPS ratio. Our preliminary dynamic light scattering experiments indicate a similar effect for rBPI$_{21}$ on membranes composed of anionic phospholipids (Fig. 6). This means that not only rBPI$_{21}$ has the capacity of forming aggregates at a low molar ratio but also that rBPI$_{21}$ is capable of cross-linking

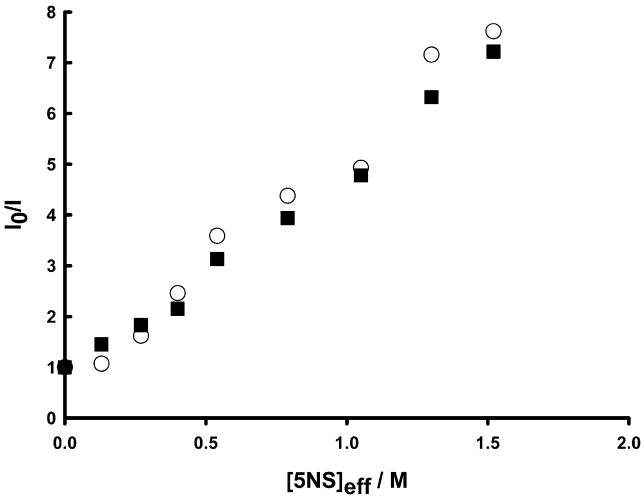

FIGURE 5 rBPI$_{21}$ location. Stern-Volmer plots for the quenching of rBPI$_{21}$ fluorescence by 5NS in POPC/POPG/LPS (○) and POPC/POPG/DAHP (■) membranes (1 mM), pH 7.4 and 37°C. Effective 5NS concentrations in the membrane were calculated as described previously (52).

TABLE 4 Location of $rBPI_{21}$ in model systems of bacterial membranes

	K_{SV} (pH 6.5)		K_{SV} (pH 7.4)	
System	5NS	16NS	5NS	16NS
POPC/POPG	2.07	0.36	0.82	1.29
POPC/POPG/DAHP	2.25	1.83	4.11	1.83
POPC/POPG/LPS	2.86	0.36	4.60	1.68

Stern-Volmer constants (K_{SV}) of $rBPI_{21}$ were obtained as described in Materials and Methods using 5NS and 16NS quenchers at 37°C, pH 6.5 and pH 7.4 Anionic lipid contents in lipid mixtures: 40% molar; LPS or DHAP content in mixtures: 5%.

LPS aggregates into larger ones. This LPS aggregation effect induced by $rBPI_{21}$ may be helpful for its in vivo function and an explanation for its high biological activity. LPS interaction with leukocytes can initiate an inflammatory responses, but the LPS that binds to BPI is essentially inactive (43). This capacity for inactivating LPS due to surface binding may help to prevent septic shock. Partially unfolded proteins are prone to aggregate. Likewise, vesicle aggregation may be a direct consequence of partial unfolding.

Role of disulfide bond in $rBPI_{21}$ interaction with model systems of bacterial membranes

As the reduction of the disulfide bond between cysteines 135 and 175 with TCP is associated with a possible conformational change of the protein in buffer, we studied this effect of the chemical change on the interaction with membranes. $rBPI_{21}$ partition to model system of bacterial membranes under physiological conditions was increased (pH 7.4, 37°C) (Table 3, Fig. 7). A fourfold increase of K_p is observed for both membranes on disulfide bond breaking. Cysteines 135 and 175 are both necessary for an efficient production of a biologically active N-terminal BPI fragment, putatively trough a disulfide bond (44), but at a certain cost in its LPS-binding activity, because disulfide bond reduction can lead to a more effective interaction with model systems of bacterial membranes.

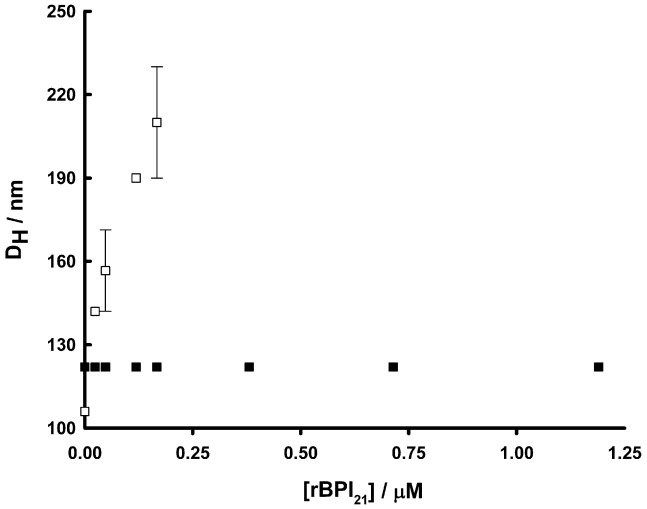

FIGURE 6 Aggregation of membrane model systems by $rBPI_{21}$. Hydrodynamic diameter variation followed by dynamic light scattering of POPC (■) and POPC/POPG (□) membranes at fixed 50 μM lipid concentration, with 45% molar of negative lipid content, in the presence of increasing $rBPI_{21}$ amount. Bars represents the size range from at least two independent experiments.

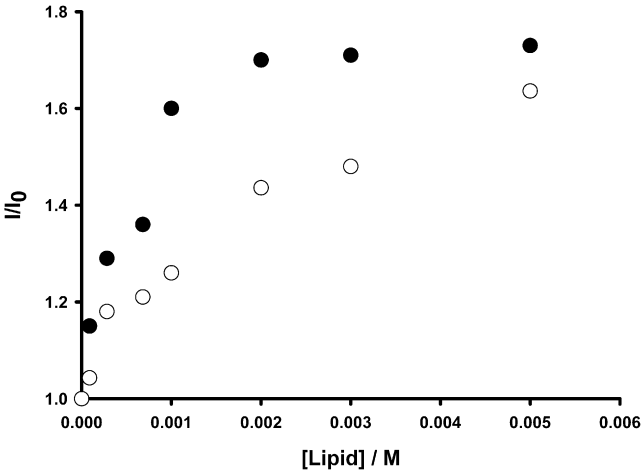

FIGURE 7 Implications of chemical modification on $rBPI_{21}$ partition to model system of bacterial membranes. $rBPI_{21}$ was dissolved in acetate buffer at pH 7.4 to a final protein concentration of 7.7 μM, and incubated with TCP 1.4 mM before partition coefficients determination, at 37°C. Partition curves of $rBPI_{21}$ to POPC/POPG/DAHP LUV with (●) and without (○) pre-incubation with TCP. K_p values are obtained by fitting the experimental data with Eq. 2.

The results are in agreement with a model of action that involves unfolding/denaturation on interaction with in LPS-containing membranes. A decrease in stability renders the membrane disturbing effect more effective.

Conformational changes of $rBPI_{21}$ after binding to lipid membranes

According to the CD measurements, $rBPI_{21}$ adopts a tridimensional conformation with regular secondary structure in aqueous buffer solution but forming a partial or total unfolded structure in the presence of liposomes composed of POPC/POPG/LPS, either at pH 6.5 or 7.4, at 25°C and 37°C (Fig. 8). The CD spectra of $rBPI_{21}$ in aqueous solution, both at pH 6.5 and pH 7.4, at 25°C and 37°C, are similar and display a positive ellipticity maximum near 194 nm and a negative ellipticity minimum around 217 nm, evidence for the presence of β-sheet conformation. In fact, secondary structure estimation from CD spectra analysis showed 33% of β-sheet, 14% of α-helix, and 30% random coil. Using POPC/POPG/LPS 0.1 mM as a bacterial membrane mimicking environment, $rBPI_{21}$ completely loses its ordered native conformation independently of the pH and/or temperature (Fig. 8). CD spectra analysis showed a loss of secondary structure, with a major decrease in the α-helix content. For $rBPI_{21}$ in interaction with POPC/POPG model systems of membranes, a less intense positive and negative ellipticity

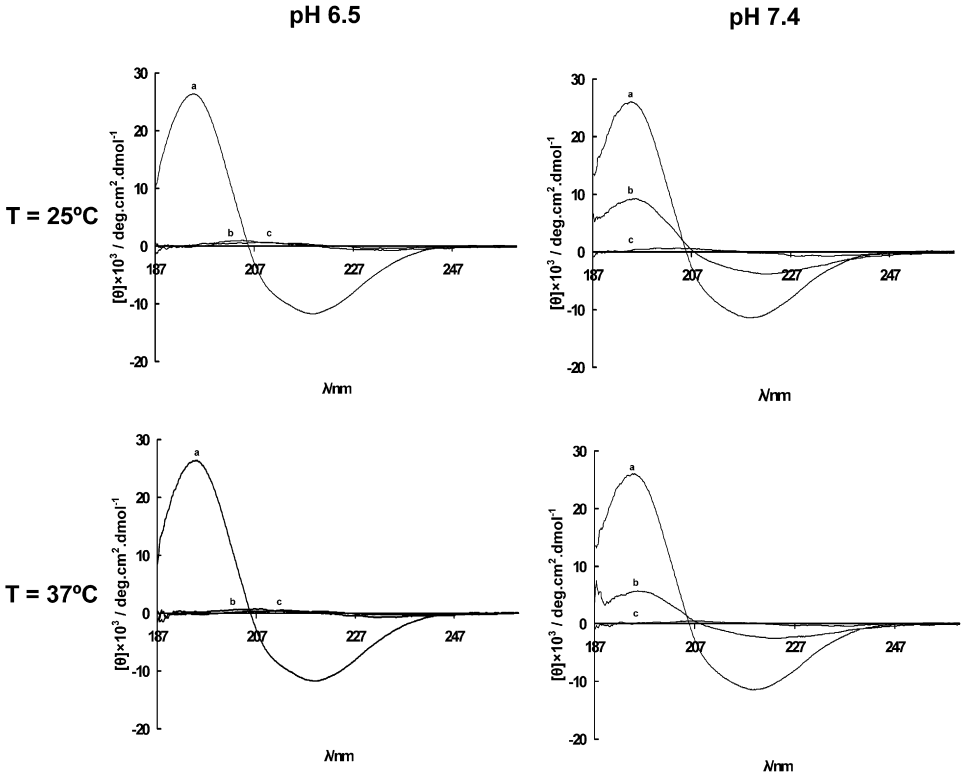

FIGURE 8 Effect of pH, temperature and lipid system on the secondary structure of $rBPI_{21}$. $rBPI_{21}$ was dissolved in phosphate buffer (pH 6.5 or 7.4), at 25°C or 37°C, to a final concentration of 7.7 μM with or without added lipid (0.1 mM). CD spectra of $rBPI_{21}$ in (*a*) buffer solution, and in interaction with (*b*) POPC/POPG/DAHP or (*c*) POPC/POPG/LPS membranes both at pH 6.5 and 7.4, and $T = 25$°C and 37°C.

and wavelengths slightly different from the ones observed in aqueous solution were observed in CD spectra.

Typically, peptides such as antimicrobial peptides, for instance, adopt a helical structure when interacting with lipid vesicles and not the other way around. Nevertheless, this high structure flexibility and low chemical conformational stability probably imply the loss of the hydrophobic pocket, because it is composed mainly by α-helix (44), which decreases in proportion with its increasing contact with lipid membranes. This represents further evidence that the exposure of this segment (hidden in the three-dimensional structure of $rBPI_{21}$ in the aqueous phase) is a key-step in an innovative model mechanism for peptide-membrane interaction. The exposure of this segment to membranes decreases the mean fluorescence lifetime of $rBPI_{21}$ (Table 1), which implies that Trp environment changes to a more hydrophilic one. Moreover, this flexibility may be the reason why $rBPI_{21}$ can coat LPS containing vesicles and, consequently, be effective in inactivating the inflammatory cascade in vivo, in a first stage.

CONCLUSIONS

We have shown that $rBPI_{21}$ in solution is stable at 37°C and has a higher chemical conformational stability at pH 7.4, when compared with a more acidic pH. It undergoes conformational changes when its disulfide bond is broken or pH decreases, exposing its Trp to a more hydrophilic environment when both changes occur. When in interaction with model systems of membranes, $rBPI_{21}$ interacts preferentially with rigid negatively charged membranes, this being one of the reasons that may be invoked for its preference for gram-negative bacteria. Also, $rBPI_{21}$ has a shallow location and completely loses its secondary structure, unfolding, while coating and aggregating LPS-containing vesicles (Fig. 8). $rBPI_{21}$ is at variance with most of antimicrobial peptides that adopt a helical structure when inserted in the lipid bilayer. This may be related to a peculiar mechanism of action, where coating and aggregation of LPS-containing entities is of first importance for their neutralization. We have also shown that decreasing the pH, near the pK_a of His, is important for $rBPI_{21}$ interaction with membranes and that the breaking of the disulfide bond may enhance its LPS-binding activity in vivo, as a consequence of a significant increase of partition coefficients. Although there are some studies of $rBPI_{21}$ in interaction with lipid systems (23,24), to our knowledge no one has identified specific amino acid residues implication in this process.

The CD spectra results have shown that $rBPI_{21}$ has a predominant β-sheet secondary structure content. The results on chemical conformational stability at pH 7.4 and 6.5 contribute to explain the partial and total loss of structure of $rBPI_{21}$ after binding to POPC/POPG/LPS liposomes at pH 7.4 and 6.5, respectively. The lower $rBPI_{21}$ conformational stability value at pH 6.5 completely agrees with a higher loss of structure. Moreover, partial or total unfolded proteins are prone to form aggregates, which could explain liposome aggregation in the presence of $rBPI_{21}$.

In summary, the results of this study highlight structural reasons that may be responsible for the selectivity of $rBPI_{21}$ for Gram-negative bacteria and show that unfolding at the surface of the membrane, on interaction with LPS is an uncommon key-event of its mechanism (Fig. 9). Antimicrobial peptides are portrayed usually as molecules unstructured in solution, which gain structure when in contact with the membrane. Peptide-peptide interactions are then triggered at certain critical concentrations (45–51), which lead to supramolecular entities that cause lysis, such as a variety of pore-forming structures. $rBPI_{21}$ seems to be quite peculiar as its mode of action is not at all related to this sequence of events from the start. It loses structure and stability on contact with LPS membranes and is able to cause membrane aggregation, which is quite perturbing for membranes and ultimately responsible for the bactericidal activity of this drug.

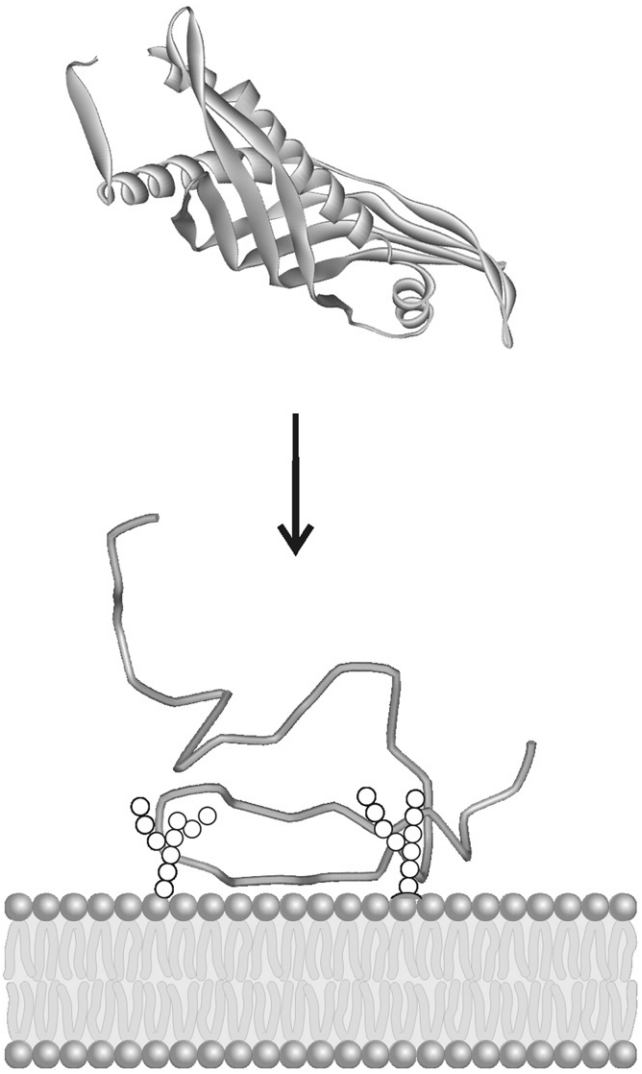

FIGURE 9 Schematic representation of the proposed mechanism of action of $rBPI_{21}$ protein. The protein interacts superficially with LPS-rigid regions of the membrane of gram-negative bacteria. This interaction is followed by the unfolding of the protein covering the surface of the cell, leading to severe membrane perturbation.

We thank XOMA for a kind gift of $rBPI_{21}$ and Prof. Amélia Pilar Rauters (Faculty of Science, University of Lisbon) for DAHP synthesis.

M.M.D. acknowledges Fundação para a Ciência e a Tecnologia do Ministério da Ciência, Tecnologia e Ensino Superior (Portugal) for fellowship SFRH/BD/41750/2007.

REFERENCES

1. Raetz, C. R., and C. Whitfield. 2002. Lipopolysaccharide endotoxins. *Annu. Rev. Biochem.* 71:635–700.
2. Rietschel, E. T., T. Kirikae, F. U. Schade, U. Mamat, G. Schmidt, et al. 1994. Bacterial endotoxin: molecular relationships of structure to activity and function. *FASEB J.* 8:217–225.
3. Hancock, R. E., and D. S. Chapple. 1999. Peptide antibiotics. *Antimicrob. Agents Chemother.* 43:1317–1323.
4. Wu, M., E. Maier, R. Benz, and R. E. Hancock. 1999. Mechanism of interaction of different classes of cationic antimicrobial peptides with planar bilayers and with the cytoplasmic membrane of *Escherichia coli*. *Biochemistry.* 38:7235–7242.
5. Chaby, R. 2004. Lipopolysaccharide-binding molecules: transporters, blockers and sensors. *Cell. Mol. Life Sci.* 61:1697–1713.
6. Schumann, R. R. 1992. Function of lipopolysaccharide (LPS)-binding protein (LBP) and CD14, the receptor for LPS/LBP complexes: a short review. *Res. Immunol.* 143:11–15.
7. Wright, S. D., R. A. Ramos, P. S. Tobias, R. J. Ulevitch, and J. C. Mathison. 1990. CD14, a receptor for complexes of lipopolysaccharide (LPS) and LPS binding protein. *Science.* 249:1431–1433.
8. Hancock, R. E. 2001. Cationic peptides: effectors in innate immunity and novel antimicrobials. *Lancet Infect. Dis.* 1:156–164.
9. Hancock, R. E., and G. Diamond. 2000. The role of cationic antimicrobial peptides in innate host defenses. *Trends Microbiol.* 8:402–410.
10. Hancock, R. E., and H. G. Sahl. 2006. Antimicrobial and host-defense peptides as new anti-infective therapeutic strategies. *Nat. Biotechnol.* 24:1551–1557.
11. Levy, O. 2000. Antimicrobial proteins and peptides of blood: templates for novel antimicrobial agents. *Blood.* 96:2664–2672.
12. Levy, O. 2004. Antimicrobial proteins and peptides: anti-infective molecules of mammalian leukocytes. *J. Leukoc. Biol.* 76:909–925.
13. Beamer, L. J., S. F. Carroll, and D. Eisenberg. 1998. The BPI/LBP family of proteins: a structural analysis of conserved regions. *Protein Sci.* 7:906–914.
14. Tobias, P. S., J. C. Mathison, and R. J. Ulevitch. 1988. A family of lipopolysaccharide binding proteins involved in responses to gram-negative sepsis. *J. Biol. Chem.* 263:13479–13481.
15. Weiss, J. 2003. Bactericidal/permeability-increasing protein (BPI) and lipopolysaccharide-binding protein (LBP): structure, function and regulation in host defense against Gram-negative bacteria. *Biochem. Soc. Trans.* 31:785–790.
16. Elsbach, P., and J. Weiss. 1998. Role of the bactericidal/permeability-increasing protein in host defense. *Curr. Opin. Immunol.* 10:45–49.
17. Weiss, J., P. Elsbach, I. Olsson, and H. Odeberg. 1978. Purification and characterization of a potent bactericidal and membrane active protein from the granules of human polymorphonuclear leukocytes. *J. Biol. Chem.* 253:2664–2672.
18. Appelmelk, B. J., Y. Q. An, B. G. Thijs, D. M. MacLaren, and J. de Graaff. 1994. Recombinant human bactericidal/permeability-increasing protein (rBPI23) is a universal lipopolysaccharide-binding ligand. *Infect. Immun.* 62:3564–3567.
19. Capodici, C., S. Chen, Z. Sidorczyk, P. Elsbach, and J. Weiss. 1994. Effect of lipopolysaccharide (LPS) chain length on interactions of

bactericidal/permeability-increasing protein and its bioactive 23-kilodalton NH2-terminal fragment with isolated LPS and intact Proteus mirabilis and Escherichia coli. *Infect. Immun.* 62:259–265.

20. Gazzano-Santoro, H., J. B. Parent, L. Grinna, A. Horwitz, T. Parsons, et al. 1992. High-affinity binding of the bactericidal/permeability-increasing protein and a recombinant amino-terminal fragment to the lipid A region of lipopolysaccharide. *Infect. Immun.* 60:4754–4761.
21. Elsbach, P. 1998. The bactericidal/permeability-increasing protein (BPI) in antibacterial host defense. *J. Leukoc. Biol.* 64:14–18.
22. Levin, M., P. A. Quint, B. Goldstein, P. Barton, J. S. Bradley, et al. 2000. Recombinant bactericidal/permeability-increasing protein (rBPI21) as adjunctive treatment for children with severe meningococcal sepsis: a randomized trial. *Lancet.* 356:961–967.
23. Wiese, A., K. Brandenburg, S. F. Carroll, E. T. Rietschel, and U. Seydel. 1997. Mechanisms of action of bactericidal/permeability-increasing protein BPI on reconstituted outer membranes of gram-negative bacteria. *Biochemistry.* 36:10311–10319.
24. Wiese, A., K. Brandenburg, B. Lindner, A. B. Schromm, S. F. Carroll, et al. 1997. Mechanisms of action of the bactericidal/permeability-increasing protein BPI on endotoxin and phospholipid monolayers and aggregates. *Biochemistry.* 36:10301–10310.
25. Rauter, A. P., S. Lucas, T. Almeida, D. Sacoto, V. Ribeiro, et al. 2005. Synthesis, surface active and antimicrobial properties of new alkyl 2,6-dideoxy-L-arabino-hexopyranosides. *Carbohydr. Res.* 340:191–201.
26. Mayer, L. D., M. J. Hope, and P. R. Cullis. 1986. Vesicles of variable sizes produced by a rapid extrusion procedure. *Biochim. Biophys. Acta.* 858:161–168.
27. Loura, L. M., A. Fedorov, and M. Prieto. 1996. Resonance energy transfer in a model system of membranes: application to gel and liquid crystalline phases. *Biophys. J.* 71:1823–1836.
28. Lakowicz, J. 1999. Principles of Fluorescence Spectroscopy, 2nd ed. Academic/Plenum Publishers, New York.
29. Santos, N. C., M. Prieto, and M. A. R. B. Castanho. 2003. Quantifying molecular partition into model systems of biomembranes: an emphasis on optical spectroscopic methods. *Biochim. Biophys. Acta.* 1612: 123–135.
30. Castanho, M. A., and M. J. Prieto. 1998. Fluorescence quenching data interpretation in biological systems. The use of microscopic models for data analysis and interpretation of complex systems. *Biochim. Biophys. Acta.* 1373:1–16.
31. Castanho, M., and M. Prieto. 1995. Filipin fluorescence quenching by spin-labeled probes: studies in aqueous solution and in a membrane model system. *Biophys. J.* 69:155–168.
32. Lehrer, S. S. 1971. Solute perturbation of protein fluorescence. The quenching of the tryptophyl fluorescence of model compounds and of lysozyme by iodide ion. *Biochemistry.* 10:3254–3263.
33. Johnson, W. C. 1999. Analyzing protein circular dichroism spectra for accurate secondary structures. *Proteins.* 35:307–312.
34. Lobley, A., L. Whitmore, and B. A. Wallace. 2002. DICHROWEB: an interactive website for the analysis of protein secondary structure from circular dichroism spectra. *Bioinformatics.* 18:211–212.
35. Pace, C. N. 1986. Determination and analysis of urea and guanidine hydrochloride denaturation curves. *Methods Enzymol.* 131:266–280.
36. Santoro, M. M., and D. W. Bolen. 1988. Unfolding free energy changes determined by the linear extrapolation method. 1. Unfolding of phenylmethanesulfonyl alpha-chymotrypsin using different denaturants. *Biochemistry.* 27:8063–8068.
37. Provencher, S. W. 1982. A constrained regularization method for inverting data represented by linear algebraic or integral-equations. *Comput. Phys. Commun.* 27:213–227.
38. Provencher, S. W. 1982. Contin—a general-purpose constrained regularization program for inverting noisy linear algebraic and integral-equations. *Comput. Phys. Commun.* 27:229–242.
39. Beamer, L. J., S. F. Carroll, and D. Eisenberg. 1999. The three-dimensional structure of human bactericidal/permeability-increasing protein: implications for understanding protein-lipopolysaccharide interactions. *Biochem. Pharmacol.* 57:225–229.
40. Myers, J. K., C. N. Pace, and J. M. Scholtz. 1995. Denaturant m values and heat capacity changes: relation to changes in accessible surface areas of protein unfolding. *Protein Sci.* 4:2138–2148.
41. Snyder, S., D. Kim, and T. J. McIntosh. 1999. Lipopolysaccharide bilayer structure: effect of chemotype, core mutations, divalent cations, and temperature. *Biochemistry.* 38:10758–10767.
42. Tobias, P. S., K. Soldau, N. M. Iovine, P. Elsbach, and J. Weiss. 1997. Lipopolysaccharide (LPS)-binding proteins BPI and LBP form different types of complexes with LPS. *J. Biol. Chem.* 272:18682–18685.
43. Leeuwenberg, J. F., M. A. Dentener, and W. A. Buurman. 1994. Lipopolysaccharide LPS-mediated soluble TNF receptor release and TNF receptor expression by monocytes. Role of CD14, LPS binding protein, and bactericidal/permeability-increasing protein. *J. Immunol.* 152: 5070–5076.
44. Beamer, L. J., S. F. Carroll, and D. Eisenberg. 1997. Crystal structure of human BPI and two bound phospholipids at 2.4 angstrom resolution. *Science.* 276:1861–1864.
45. Almeida, P. F., and F. W. Wiegel. 2006. A simple theory of peptide interactions on a membrane surface: excluded volume and entropic order. *J. Theor. Biol.* 238:269–278.
46. Huang, H. W. 2006. Molecular mechanism of antimicrobial peptides: the origin of cooperativity. *Biochim. Biophys. Acta.* 1758:1292–1302.
47. Huang, H. W., F. Y. Chen, and M. T. Lee. 2004. Molecular mechanism of peptide-induced pores in membranes. *Phys. Rev. Lett.* 92:198304.
48. Melo, M. N., and M. A. Castanho. 2007. Omiganan interaction with bacterial membranes and cell wall models. Assigning a biological role to saturation. *Biochim. Biophys. Acta.* 1768:1277–1290.
49. Pan, Y. L., J. T. Cheng, J. Hale, J. Pan, R. E. Hancock, et al. 2007. Characterization of the structure and membrane interaction of the antimicrobial peptides aurein 2.2 and 2.3 from Australian southern bell frogs. *Biophys. J.* 92:2854–2864.
50. Pott, T., M. Paternostre, and E. J. Dufourc. 1998. A comparative study of the action of melittin on sphingomyelin and phosphatidylcholine bilayers. *Eur. Biophys. J.* 27:237–245.
51. Weiss, T. M., L. Yang, L. Ding, A. J. Waring, R. I. Lehrer, et al. 2002. Two states of cyclic antimicrobial peptide RTD-1 in lipid bilayers. *Biochemistry.* 41:10070–10076.
52. Santos, N. C., M. Prieto, and M. A. Castanho. 1998. Interaction of the major epitope region of HIV protein gp41 with membrane model systems. A fluorescence spectroscopy study. *Biochemistry.* 37: 8674–8682.